Available online at www.sciencedirect.com
ScienceDirect
Bioorganic & Medicinal Chemistry 15 (2007) 2016–2023
Bioorganic & Medicinal Chemistry

Cell-penetrating autoantibody induces caspase-mediated apoptosis through catalytic hydrolysis of DNA

Eun-Jung Lee,[a] Eun-Jung Jang,[a] Eunhae Lee,[b] Jaehoon Yu,[b] Hee Yong Chung[c] and Young-Ju Jang[a,*]

[a]*Laboratory of Immunology, Institute for Medical Science and BK 21 Program, Ajou University, School of Medicine, Suwon 443-721, Republic of Korea*
[b]*Department of Chemistry and Education, Seoul National University, Seoul 151-742, Republic of Korea*
[c]*Department of Microbiology, Hanyang University College of Medicine, Seoul 133-791, Republic of Korea*

Received 9 November 2006; revised 22 December 2006; accepted 23 December 2006
Available online 30 December 2006

Abstract—In the present study, we investigated the substrate specificity of catalytic activity of a cytotoxic anti-DNA monoclonal autoantibody, G1-5, which was obtained from an MRL-*lpr*/*lpr* mouse by hybridoma technology. The antibody catalyzed hydrolysis of single- and double-stranded DNA with a higher substrate specificity for thymine than adenine by either β-glycosidic or phosphodiester bond cleavage. The hydrolysis rate (k_{cat}) showed maximum at acidic pH conditions, suggesting that the catalytic site of the antibody contains essential carboxylic group(s). Treatment of cells with the antibody promoted cell death and induced the activation of caspases. The cell death induced by the antibody was inhibited by the pan-caspase inhibitor. Furthermore, the antibody binds to cell membrane and penetrates into the cells. Our results suggest that the cell death is initiated by antibodies penetrating to cells and nucleus, hydrolyzing considerable amount of DNA, and mediating the caspase-dependent apoptotic pathway.

1. Introduction

Circulating autoantibodies that interact with DNA are a typical feature of systemic lupus erythematosus (SLE) in humans and MRL-*lpr*/*lpr* mice.[1] Some anti-DNA autoantibodies have been known to have nuclease or protease activity as well as cytotoxicity in vitro.[2,3]

Antibodies (Abs) with nuclease or protease activities, known as catalytic Abs, are found in autoimmune-prone mice more frequently than in normal mice,[4,5] suggesting that catalytic activity participates in the unique function and pathogenesis of autoantibodies. Catalytic Abs have been generated by in vitro immunization in autoimmune-prone and normal mice using transition state analogs as haptens.[6] Antibodies against these haptens could catalyze hydrolysis of the intended nuclease or protease activities.[7] Natural autoantibodies also showed the same enzymatic activities.[8,9] However, the fine structural properties of chemical bonds in DNA substrates that hydrolyzed by anti-DNA autoantibodies isolated from SLE-prone humans or animals have not been reported except one case. Our group previously produced several anti-double-stranded (dsDNA) monoclonal autoantibodies from an MRL-*lpr*/*lpr* mouse[10] and reported that one of the autoantibodies, G1-2, has catalytic activities, with a preference for the hydrolysis of β-glucosidic bonds.[8]

Besides the catalytic activity, there are other interesting features of the anti-DNA autoantibodies that may participate in their pathogenic effects. Autoantibodies such as anti-DNA and anti-RNP can penetrate into living cells and interact with their intracellular and nuclear targets.[11–14] Some of these autoantibodies possess multiple positively charged amino acids in the complementarity determining region 3 of H chain (CDR3H) in a sequence that resembles a nuclear localization signal.[15] Several studies have demonstrated that the cell penetrating Abs can induce tumor cell death.[16] Most of these studies, however, have been performed using polyclonal anti-DNA Abs that have heterogeneous binding properties and functions. Recently, however, monoclonal antibodies (mAbs) have been utilized for studying the

Keywords: Anti-DNA autoantibody; Catalytic activity; Glycosidic bond; Phosphodiester bond; Cytotoxicity.
* Corresponding author. Tel.: +82 31 219 4516; fax: +82 31 219 4401; e-mail: jangyj@ajou.ac.kr

0968-0896/$ - see front matter © 2006 Elsevier Ltd. All rights reserved.
doi:10.1016/j.bmc.2006.12.037

involvement of signal pathways in penetrating anti-DNA antibody-induced apoptosis.[17] Studies using mAbs are necessary to more clearly determine not only the mechanisms of cell death but also details of DNA hydrolysis induced by anti-DNA autoantibodies. Such studies are important because cytotoxic anti-DNA antibodies are currently of great interest in the fields of autoimmunity and cancer therapy.

In the present study, we not only measured the catalytic properties of mAb G1-5 but also studied cytotoxic mechanisms, because G1-5 showed the highest cytotoxic activity for several cancer cell-lines among various mAbs we produced. By analyzing catalytic activities of DNA hydrolysis and mechanisms of cell death induced by anti-DNA autoantibodies using G1-5, we propose that the autoantibodies penetrate into the cells and hydrolyze DNA and induce caspase-mediated apoptosis.

2. Results and discussion

2.1. DNA hydrolyzing activity of anti-DNA monoclonal autoantibody G1-5

We examined the ability of mAb G1-5 to hydrolyze dsDNA using plasmid pUC18 and double-stranded M13mp18 as substrates. As shown in Figure 1a, G1-5 IgG (100 μg/ml) transformed the supercoiled pUC18 into an open circular form and cleaved the M13mp18 in 3 h. Fab (100 μg/ml) produced by papain digestion of G1-5 IgG also hydrolyzed both pUC18 and M13mp18 DNA, although the activity was lower than that of the intact IgG. When pUC18 DNA was treated with various concentrations of mAb G1-5, the cleaving activity of the Ab was observed at an even lower concentration (30 μg/ml), and some open circular DNA was converted to the linear form by 300 μg/ml G1-5 (Fig. 1b). Also, hydrolysis of pUC18 DNA was time-dependent (Fig. 1c). In addition, the supercoiled form of pUC18 was reduced starting after 1 h of incubation and disappeared completely after 6 h, and the linear form appeared after 6 h or more of incubation.

2.2. Substrate specificity of enzymatic activity

To further analyze the DNA hydrolyzing activity of mAb G1-5, we initially measured the cleavage of the digoxigenin-labeled single-stranded oligonucleotides ($(dA)_{40}$ or $(dT)_{40}$) and double-stranded oligonucleotides($(dA)_{40}$:$(dT)_{40}$). The Ab hydrolyzed both ssDNA and dsDNA substrates with sequence preference for thymine over adenine (Fig. 2a). We also investigated the cleavage of the same oligonucleotides by S1 nuclease and DNase I. S1 nuclease cleaved both $(dA)_{40}$ and $(dT)_{40}$ without a clear sequence specificity (Fig. 2b). Whereas DNase I showed remarkable cleaving activity against $(dA)_{40}$:$(dT)_{40}$, it cleaved either $(dA)_{40}$ or $(dT)_{40}$ at lower levels (Fig. 2c). By showing a difference of the substrate specificity between mAb G1-5 and DNases, we could eliminate a possibility of contaminations of the purified antibody with natural enzymes. To examine the activity in greater detail, we also measured the glycosidase and phosphatase activities of the Ab using various DNA substrates (Fig. 3a) and used the results to calculate their kinetic constants (Table 1). Although the k_{cat} and K_m values were not as efficient as natural enzymes, mAb G1-5 showed clearly glycosidase and phosphatase activities toward a variety of substrates. Both the glycosidase and phosphatase showed saturation kinetics. As demonstrated by the highest k_{cat}/K_m value, the Ab had the highest catalytic specificity for *p*NP-β-Gal for glycosidase activity, which has a same β-anomer as the C–N glycosidic bond in DNA. The maximum activity was observed at pH 4–4.8, suggesting the presence of an essential carboxylic group(s) in the catalytic site of the Ab (Fig. 3b). Figure 3c shows a typical Lineweaver–Burk plot used to calculate the kinetic constants.

The mAb G1-5 has glycosidase and phosphatase activities toward both dsDNA and ssDNA with a higher specificity for thymine than adenine. The ability to cleave glycosidic and phosphodiester bonds of DNA might be an intrinsic property of anti-DNA Abs, because these chemical bonds are the most frequent in DNA. The exertion of the glycosidase activities toward specific DNA structure such as C–N glycosidic bond by mAb G1-5 might partly contribute to DNA

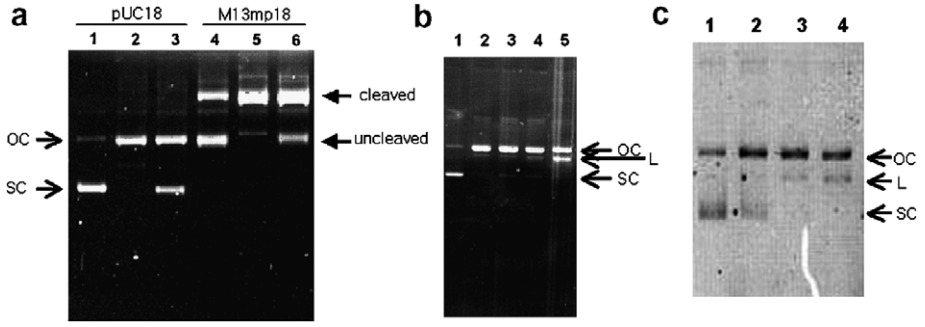

Figure 1. Cleavage of supercoiled pUC18 DNA or M13mp18 dsDNA by mAbG1-5. (a) pUC18 or M13mp18 dsDNA (1 μg) was incubated without (lanes 1 and 4) or with 100 μg/ml of G1-5 IgG (lanes 2 and 5) or G1-5 Fab (lanes 3 and 6) for 3 h. (b) pUC18 DNA (1 μg) was incubated with 0 (lane 1), 30 (lane 2), 50 (lane 3), 100 (lane 4) or 300 (lane 5) μg/ml G1-5 for 3 h. (c) pUC18 DNA (1 μg) was incubated for 1, 3, 6, or 16 h (lanes 1–4, respectively) with 100 μg/ml G1-5. SC, OC, and L represent supercoiled, open circular, and linear forms of plasmid DNA, respectively.

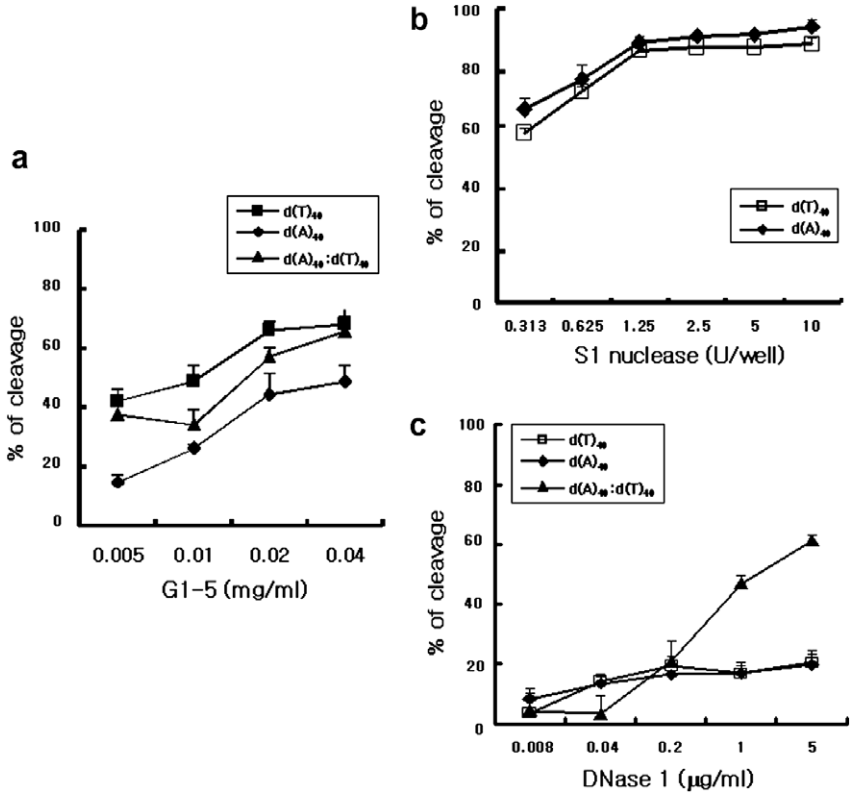

Figure 2. ALONA of mAb G1-5 and natural DNases. Double-labeled (5′-digoxigenin and 3′-biotin) single-stranded 40-mer $(dA)_{40}$ or $(dT)_{40}$ and double-stranded 40-mer $(dA)_{40}$:$(dT)_{40}$ immobilized on a streptavidin-coated microtiter plate was used as DNA substrates. The amount of uncleaved DNA after treatment of mAb G1-5 (a), S1 nuclease (b), or DNase I (c) was determined as explained in Section 4. The results are presented as the percentage of cleavage in the absence of added G1-5 and are means ± SD of triplicate measurements.

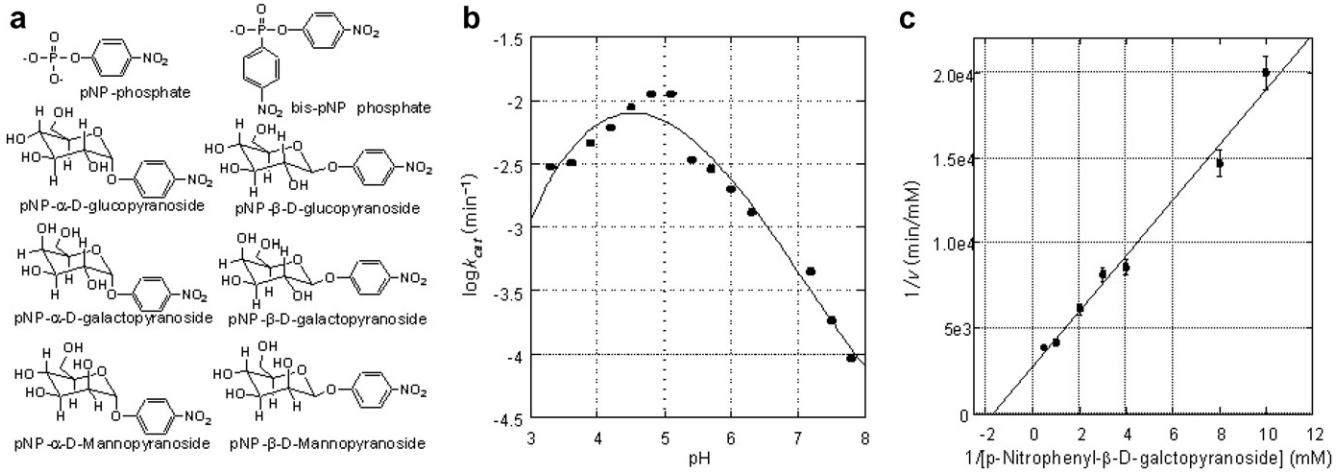

Figure 3. (a) Structure of DNA substrates used for studying the catalytic activities of G1-5. (b) The pH dependence of the catalytic activity (k_{cat}) of G1-5 for pNP-β-Gal. (c) A typical Lineweaver–Burk plot to determine the V_{max} and K_m values. Substrate is pNP-β-Gal.

cleavage-mediated cell death, leading to tissue damage in autoimmune disease. We also showed that an essential carboxylic group(s) might be present in the catalytic site of the Ab by the observation that the catalytic activity was optimal under acidic conditions. The carboxylic acid moieties of the Glu residues in CDR3H, CDR2 of light chain (CDR2L), and CDR3L of mAb G1-5 (Fig. 4) may contribute to the hydrolyzing ability by functioning as general acid–bases. It is worth being explored clearly whether the acidic amino acids contribute to the catalytic activity, contrary to the fact that the positively charged amino acid residues play a role in DNA binding[1,18] by studies such as site-directed mutagenesis and computer-modeling.

Catalytic properties of mAb G1-5 are quite different from those of mAb G1-2[8], which has very high sequence identity with mAb G1-5 (Fig. 4). First, the k_{cat} values of

Table 1. Catalytic constants of Ab G1-5 for various substrates

Substrate	V_{max} (M/min)	k_{cat} (min^{-1})	K_m (μM)	k_{cat}/K_m (M^{-1} min^{-1})	Reference
p-Nitrophenyl-α-D-glucopyranoside (*p*NP-α-Glc)	—	—	—	—	ND
p-Nitrophenyl-β-D-glucopyranoside (*p*NP-β-Glc)	9.3×10^{-11}	1.5×10^{-4}	2.1×10^{2}	0.71	pH 5.0
*p*NP-α-galactopyranoside (Gal)	2.7×10^{-10}	4.2×10^{-4}	2.0×10^{2}	2.1	pH 5.0
*p*NP-β-Gal	1.2×10^{-9}	1.8×10^{-3}	2.3×10^{2}	7.8	pH 5.0
*p*NP-α-mannopyranoside (Man)	4.0×10^{-10}	4.8×10^{-4}	5.9×10^{2}	0.81	pH 5.0
*p*NP-β-Man	—	—	—	—	ND
p-Nitrophenyl phosphate (pNPP)	1.1×10^{-9}	1.8×10^{-3}	3.8×10^{2}	4.7	pH 5.0
	1.3×10^{-9}	2.0×10^{-4}	1.4×10^{3}	0.14	pH 7.5
Bis-pNPP	—	—	—	—	ND

ND, not detected. The assay was carried out at 37 °C with 0.094 mg/mL G1-5 in 10 mM MES (pH 5) with 150 mM NaCl.

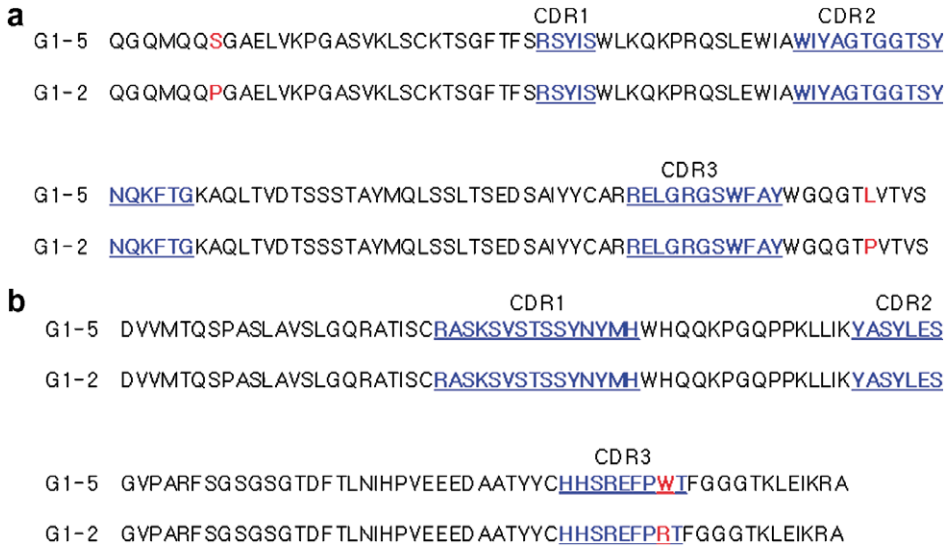

Figure 4. Alignment of amino acid sequences of the VH (a) and VL regions (b) of G1-5 and G1-2. Different amino acids and CDR regions are shown in red and underlined in blue, respectively. The GenBank Accession Nos. are AF289182 (G1-5VH), AF289183 (G1-5 VL), AF289180 (G1-2 VH), and AF289181 (G1-2 VL).

mAb G1-5 are about an order of magnitude lower than those of mAb G1-2. Second, mAb G1-5 accepts both α- and β-anomeric carbohydrates as substrates, whereas mAb G1-2 is specific for β-anomeric substrates. Third, the best substrates for mAbs G1-5 and G1-2 are β-galactoside and β-glucoside, respectively. The phosphatase activity of mAb G1-5 is also an order of magnitude lower than that of mAb G1-2. Interestingly, there are only a few different amino acids between the two Abs (one in CDR3-VL, one in FR1-VH, and one in FR4-VH, presented as red colored letters in Fig. 4), although they have quite different catalytic activities. This may be due to a relatively large conformational change in the Abs as a result of mutations in the FR.[19] Similar findings were also previously reported for glycosidase antibodies differing by only four amino acids in the FR.[6] It is suggested that anti-DNA autoantibodies found in the sera of SLE patients and MRL-*lpr*/*lpr* mice have distinct abilities to cleave DNA even at the level of fine difference of chemical bonds and forms.

2.3. Analysis of cell death induced by mAb G1-5

We analyzed cytotoxicity of the Ab in the range of 30–1000 μg/ml in several cell lines (HL60, L929, Jurkat, and HeLa) (Fig. 5). Cell death rates of the cell lines were not so high even at the high concentration of the antibody. However, HL60 cells were the most sensitive to the Ab-induced cytotoxicity. From 200 μg/ml of the Ab, approximately 30–35% of the HL60 cells were dead. Normal mouse IgG was not cytotoxic to these cell lines even at 1000 μg/ml (data not shown). To determine whether caspases are involved in the cell death induced by the Ab, we examined caspase-3 activation and cleavage of PARP, an endogenous substrate of caspase-3. When HL60 cells were treated with the Ab, both caspase-3 activation and PARP cleavage were detected within 48 h (Fig. 6a). Activations of caspase-3 and -7 were also analyzed by fluorescence intensities (Fig. 6b). Both mAb G1-5 and sTRAIL, a well-known inducer of caspase activation, activated caspase-3/7, whereas cells cultured in the absence of either reagent did not activate them. The levels of caspase-3/7 activation and PARP cleavage induced by the mAb, however, were lower than those induced by sTRAIL. One of the possible reasons might be the lower level of cell death induced by the mAb G1-5. Next, we tested the effect of zVAD-fmk, a pan-caspase inhibitor, on mAb G1-5-induced cell death. As shown in Figure 6c, zVAD-fmk dose-dependently inhibited both sTRAIL- and mAb G1-5-induced

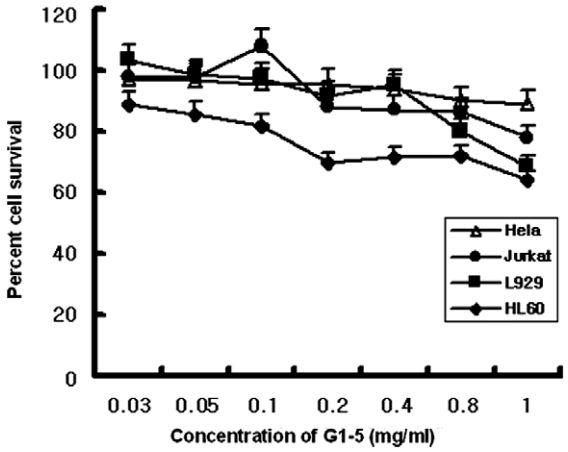

Figure 5. Cytotoxicity of mAb G1-5 against various cell lines. Percentage survival was determined by CCK-8 assay after incubation of each cell line with indicated concentrations of G1-5 for 24 h. The extent of cell survival after a 24-h culture without Ab, but with the same volume of Ab dilution buffer, phosphate-buffered saline (PBS) was regarded as 100%. Results shown are means ± SD of at least triplicate measurements.

death of HL60 cells, although the level of the inhibition by zVAD-fmk was relatively lower in case of treatment of the Ab. These results suggest that the mechanism of cell death induced by mAb G1-5 includes the activation of caspases in some extent.

The mAb G1-5 induced cell death by mechanisms involving activation of caspases. These findings are essentially in agreement with recent reports showing the importance of caspases in anti-DNA Ab-induced apoptosis.[17] Similarly, cytotoxic Abs against recoverin also induced the death of retinal cells by activating a caspase 3-dependent apoptosis pathway.[20] However, we could not exclude involvement of other mechanisms such as caspase-independent apoptosis for following reasons; compared to the experiments performed with sTRAIL, the mAb G1-5 did not fully activate caspases, and the cell death induced by the mAb was not completely inhibited by a pan-caspase inhibitor.

From above results, two mechanisms are suggested in G1-5-induced cell death. First, upon penetrating the cells, mAb G1-5 enters the nucleus, where it cleaves DNA due to enzymatic activities, such as glycosidase or phosphatase, resulting in cell death. Second, the mAb induces cell death by triggering a signal transduction pathway (at least partly caspase-dependent) upon binding to the cell membrane. It is possible that the two mechanisms may work together to cause cell death as suggested in recent report.[17] Further analysis of the DNA-hydrolyzing and cytotoxic activities of anti-DNA antibodies will lead to a better understanding of the mechanism of tissue damage and pathogenesis of autoimmune diseases such as SLE.

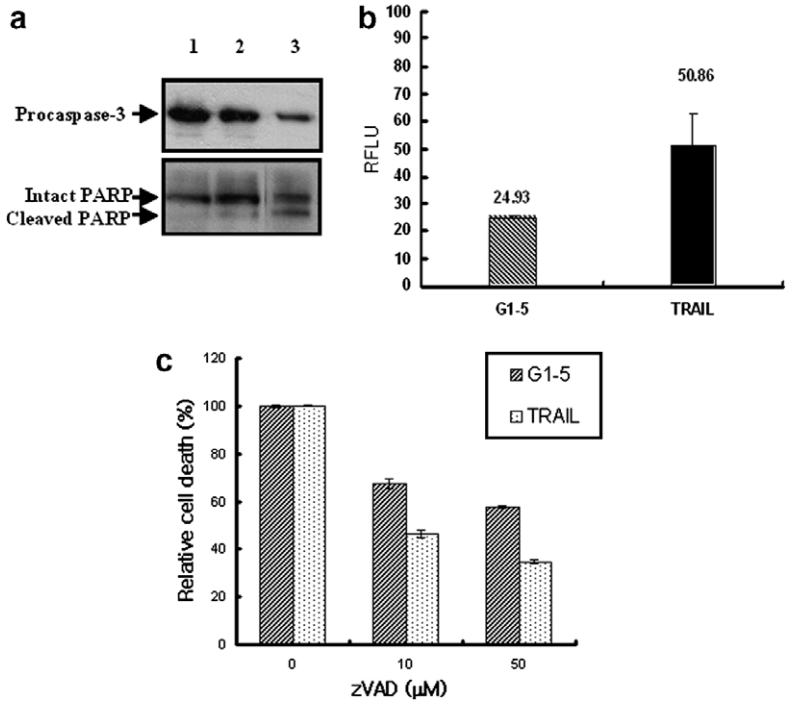

Figure 6. (a) Caspase-3 activation and PARP cleavage in HL60 cells treated with mAb G1-5 or sTRAIL. Cells were cultured in the absence (lane 1) or presence of 100 μg/ml G1-5 (lane 2) or 1 μg/ml sTRAIL (lane 3) for 24 h. Cells were lysed in Laemmli sample buffer. Samples were normalized for total protein content and were analyzed by Western blotting. (b) After a 24-h treatment with 100 μg/ml G1-5 or 1 μg/ml sTRAIL, caspase 3/7 activity was measured in the cell culture supernatant using ApoONE homogeneous caspase-3/7 assay reagents and a fluorometric plate reader. The activity is presented as the relative fluorescence units (RFLU) compared to cells incubated with the same volume of PBS (buffer used for dilution of G1-5 or sTRAIL). (c) Effects of zVAD-fmk on the cytotoxicity of G1-5 or sTRAIL in HL60 cells. Cells (4×10^4) were treated with 100 μg/ml G1-5 or 1 μg/ml sTRAIL for 24 h in the presence of the indicated concentrations of zVAD-fmk. Cell viability was measured by CCK-8 assay. Results shown are means ± SD of triplicate measurements.

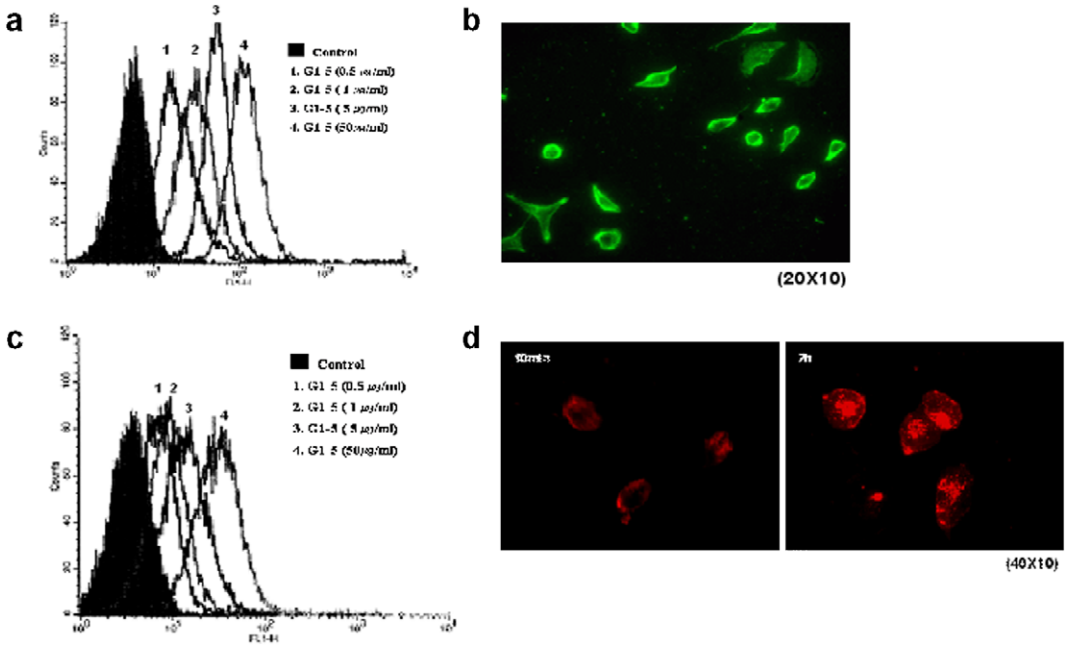

Figure 7. (a) Analysis of cell surface binding of G1-5 by FACS. After incubation of HL60 cells with various concentrations of G1-5 at 4 °C for 3 h, the cells were harvested, washed extensively, and fixed. Bound G1-5 was detected with fluorescein-EX-conjugated anti-mouse IgG using flow cytometer. HL60 cells incubated with fluorescein-EX-anti mouse IgG alone were used as a control (filled bars). (b) Analysis of cell surface binding of G1-5 by fluorescence microscopy. Image of L929 cells treated with 50 μg/ml of rhodamine Red-X-labeled G1-5 at 4 °C for 2 h (200× magnification). (c) Analysis of internalization of G1-5 into cells by FACS. HL60 cells were cultured at 37 °C for 2 h in the presence of various concentrations of G1-5 labeled with fluorescein-EX. Cells incubated with PBS alone were used as control (filled bars). (d) Analysis of internalization of G1-5 into cells by fluorescence microscopy. Images of L929 cells treated with 50 μg/ml of rhodamine Red-X-labeled G1-5 at 37 °C for 10 min (left) or 2 h (right) (400× magnification).

2.4. Cell surface binding and intracellular localization of mAb G1-5

We next determined whether the mAb could bind to the cell surface and enter the cells. First, to examine the binding of the mAb to the cell surface, we incubated HL60 cells with mAb G1-5 at 4 °C. The bound G1-5 was detected with fluorescein-EX-conjugated anti-mouse IgG and performed flow cytometric analysis. As shown in Figure 7a, mAb G1-5 bound to cell surface in a dose-dependent manner from 0.5 up to 50 μg/ml. To examine whether the mAb enters the cells, we cultured HL60 cells in the presence of fluorescein-EX-labeled G1-5 at 37 °C. We found that the level of mAb G1-5 internalization increased with the concentration of Ab in the range of 0.5–50 μg/ml (Fig. 7c). Cell surface binding and intracellular localization of the Ab were confirmed using adherent cell line L929 by fluorescence microscopy. As shown in Figure 7b, when L929 cells were treated with 50 μg/ml Rhodamine red-X-labeled G1-5 for 2 h at 4 °C, binding of the Ab to the cell surface could be detected. As shown in Figure 7d, when the L929 cells were incubated with the Rhodamine red-X-labeled G1-5 at 37 °C, the Ab could be found inside the cells within 10 min, although the level of inside Abs was low. After 2 h, there were higher amounts of the internalized Abs, and some of the labeled Abs were present in the nucleus.

The mAb G1-5 entered the cells and was located in the nucleus. It has been shown that the nuclear localizing anti-DNA Abs from SLE patients contain multiple positively charged amino acids in the CDRs in a sequence that resembles a nuclear localization signal.[15] In fact, mAb G1-5 has several Arg or Lys residues in the CDR1-VH, CDR2-VH, CDR3-VH, CDR1-VL, and CDR3-VL regions, including two adjacent Arg residues at the end of FR4 and CDR3 of VH (Fig. 4). It might be suggested that mAb G1-5 is possibly localized to the nuclear via the positively charged amino acids in the antigen binding sites, although non-penetrating Abs have also been known to contain the basic amino acids in the CDRs.[21] Penetration of autoantibodies into living cells and nuclear localization supports the possible interaction between the autoantibodies and nuclear DNA as well as the role of the autoantibody in the pathogenesis and tissue damage of autoimmune diseases.[3]

3. Conclusion

Catalytic and cytotoxic properties of anti-DNA monoclonal autoantibody, G1-5, produced from an MRL-*lpr/lpr* mouse were studied. The antibody preferentially cleaves thymine-rich single- and double-stranded DNA either by β-galactosidic or phosphodiester bond hydrolysis. The hydrolysis rate (k_{cat}) was maximized at acidic pH, suggesting that the general acid(s) is (are) involved in the catalytic core. Treatment of cells with the autoantibody promoted cell death, which is induced by the activation of caspases. Inhibition of apoptosis by a caspase inhibitor proposes a mechanism that the antibodies

enter nucleus of cells, catalyzing the hydrolysis of DNA, and then activating caspase-dependent apoptosis, resulting in cytotoxic effect.

4. Experimental

4.1. Cell culture

Cancer cell lines HL60, Jurkat, L929, and HeLa were obtained from the American Type Culture Collection. Cell lines were maintained in either Roswell Park Memorial Institute-1640 medium (HL60 and Jurkat) or Dulbecco's modified Eagle's medium (L929 and HeLa) supplemented with 10% fetal bovine serum (GIBCO BRL) and 1% penicillin/streptomycin (GIBCO BRL) in a humidified atmosphere at 37 °C and 5% CO_2.

4.2. Production of monoclonal anti-DNA mAb G1-5 IgG and G1-5 Fab fragments

We previously produced monoclonal autoantibodies that react with DNA from an MRL-*lpr*/*lpr* mouse using hybridoma technology.[10] Monoclonal IgG was purified from the culture supernatant of a hybridoma clone by protein G affinity chromatography (Amersham Biosciences) according to the manufacturer's instructions. Fab fragments were prepared by digestion of the purified mAb G1-5 IgG with papain (Sigma), followed by purification by protein G affinity chromatography as described.[22]

4.3. Cytotoxicity assay

Cell viability was measured using a Cell Counting Kit-8 (CCK-8) according to the manufacturer's instructions (Dojindo Molecular Technologies, Japan). Briefly, 100 μl of target cells (2×10^4 cells for suspension cultured cells and 6×10^3 cells for adherent cells) in the presence or absence of the Ab was added to each well of a 96-well plate (Costar), and the plate was incubated for 24 h at 37 °C in a humidified 5% CO_2 atmosphere. Following incubation, 10 μl Dojindo's tetrazolium salt, WST-8 (2-(2-methoxy-4-nitrophenyl)-3-(4-nitrophenyl)-5-(2,4-disulfophenyl)-2H-tetrazolium, monosodium salt), was added to each well for 3 h at 37 °C, and amount of the produced water-soluble formazan dye was measured at 450 nm with a microplate reader.

4.4. Analysis of DNA and oligonucleotide cleavage

Plasmid DNA (pUC18) or M13mp18 dsDNA was incubated with G1-5 IgG or G1-5 Fab in 25 mM Tris–HCl (pH 7.5) containing 10 mM $MgCl_2$. After incubation at 37 °C, DNA was separated by electrophoresis on a 1% agarose gel and stained with 0.5 μg/ml ethidium bromide.

For analyzing cleavage of dsDNA and ssDNA further, affinity-linked oligonucleotide nuclease assay was performed as described previously.[23] The 5′-digoxigenin- and 3′-biotin-labeled single-stranded oligonucleotides were obtained from Genotech. The double-stranded oligonucleotides were produced by mixing equimolar amounts of the two complementary single-stranded oligonucleotides, heating at 65 °C for 5 min, and cooling slowly to room temperature. The amount of uncleaved digoxigenin-labeled DNA was determined by adding alkaline phosphatase-labeled anti-digoxigenin Fab fragments (Roche), followed by *p*-nitrophenyl phosphate (*p*NPP) substrate (Sigma). The absorbance of the solution in each well was then determined at 405 nm with an ELISA plate reader. S1 nuclease and DNase I were purchased from Amersham Pharmacia Biotech and USB, respectively. Reaction of S1 nuclease (0.313–10 U/well) with the oligonucleotides was performed at pH 4.6 in 30 mM sodium acetate, 280 mM NaCl, and 1 mM $ZnSO_4$ for 7 min at 37 °C. DNase I (0.008–5 μg/ml) was incubated at pH 7.5 in 25 mM Tris–HCl, 10 mM $MgCl_2$ for 30 min at 37 °C.

4.5. Catalytic assays for mAb G1-5

Phosphatase activity was determined using an enzymatic assay employing *p*-nitrophenyl phosphate (*p*NPP) or bis-*p*NPP. Glycosidase activity was determined using enzymatic assays with various substrates (Sigma) which are illustrated in Figure 3a. Kinetic assays were performed in 10 mM morpholinoethane sulfonic acid (MES) (pH 3–7) or 10 mM EPPS (pH 7–8) in the presence of 0.6 mM of the Ab. Both buffers contained 100 mM NaCl, and the assays were performed at 37 °C. Product conversion was determined by measuring the amount of *p*-nitrophenol produced using an HPLC system with monitoring at 315 nm. For the HPLC, a C18 column (3.5 μm; 4.6×150 mm) was used as the stationary phase, and 50% aqueous acetonitrile containing 0.1% trifluoroacetic acid was used as the mobile phase. Kinetic data were collected under conditions where less than 1% of the substrate was converted to the product. Background hydrolysis rates were measured in the absence of the Ab and under the same conditions used for the catalytic assays.

4.6. Western blotting and fluorescent caspase assays

Western blotting was performed as described previously.[24] Abs against caspase-3 and poly (ADP-ribose) polymerase (PARP) were purchased from Stressgen and Cell Signaling Technology, respectively. Cells were plated in white 96-well plates at the density of 2×10^4 cells per well. The cells were treated with mAb G1-5 or soluble tumor necrosis factor-related apoptosis inducing ligand (sTRAIL) for 24 h at 37 °C, and caspase activity was measured using a tagged caspase substrate (rhodamine-labeled DEVD peptide) according to the manufacturer's instructions (Apo-ONE Homogeneous Caspase 3/7 Assay; Promega). The release of the fluorogenic moiety by activated caspase was measured at 485 nm using a fluorometric plate reader (LS55 luminescene spectrometer; Perkin Elmer). Treatments were performed in triplicate, and the average and standard deviation (SD) were plotted.

4.7. Cell surface binding and intracellular localization of mAb G1-5

Cell surface binding and entrance of mAb G1-5 into cells were analyzed in HL60 or L929 cells by flow

cytometry and fluorescence microscopy using FACS-Vantage (Becton–Dickinson) and Axiovert 200 (ZEISS), respectively. The mAb G1-5 and anti-mouse IgG were labeled using either fluorescein-EX (Invitrogen) or rhodamine Red TM-X (Molecular Probes). Detailed methods of indirect FITC labeling and direct rhodamine labeling are described.[25]

Acknowledgments

This work was supported by a grant from the Korea Research Foundation (MOEHRD, Basic Research Promotion Fund; KRF-2006-521-C00132) and a Grant 2006 from the Department of Medical Sciences, Graduate School of Ajou University. Support was also partly received from the KOSEF fund. E.L. is a beneficiary of the Brain Korea Program (BK21 Korea).

References and notes

1. Jang, Y. J.; Stollar, B. D. *Cell. Mol. Life Sci.* **2003**, *60*, 309–320.
2. Paul, S. *Ann. N. Y. Acad. Sci.* **1998**, *865*, 238–246.
3. Kozyr, A. V.; Sashchenko, L. P.; Kolesnikov, A. V.; Zelenova, N. A.; Khaidukov, S. V. *Immunol. Lett.* **2002**, *80*, 41–47.
4. Tawfik, D. S.; Chap, R.; Green, B. S.; Sela, M.; Eshhar, Z. *Proc. Natl. Acad. Sci. U.S.A.* **1995**, *92*, 2145–2149.
5. Yu, J.; Choi, S. Y.; Han, E. Y.; Hwang, J. S.; Seo, S. H.; Park, H.; Youn, H. J. *Mol. Cells* **1996**, *6*, 411–415.
6. Yu, J.; Choi, S. Y.; Moon, K. D.; Chung, H. H.; Youn, H. J.; Jeong, S.; Park, H.; Schultz, P. G. *Proc. Natl. Acad. Sci. U.S.A.* **1998**, *95*, 2880–2884.
7. Wentworth, P., Jr.; Liu, Y.; Wentworth, A. D.; Fan, P.; Foley, M. J.; Janda, K. D. *Proc. Natl. Acad. Sci. U.S.A.* **1998**, *95*, 5971–5975.
8. Nguyen, H. T. T.; Jang, Y. J.; Jeong, S.; Yu, J. *Biochem. Biophy. Res. Commun.* **2003**, *311*, 767–773.
9. Dubrovskaya, V. V.; Andryushkova, A. S.; Kuznetsova, I. A.; Toporkova, L. B.; Buneva, V. N.; Orlovskaya, I. A.; Nevinsky, G. A. *Biochemistry (Moscow)* **2003**, *68*, 1081–1088.
10. Park, J. S.; Kim, Y. T.; Lee, C. H.; Youn, J. K.; Jang, Y. J. *Korean J. Biol. Sci.* **1998**, *2*, 371–375.
11. Alacon-Segovia, D.; Llorente, L.; Ruiz-Argielles, A. *Immunol. Today* **1996**, *17*, 164.
12. Madaio, M. P.; Yanase, K. *J. Autoimmun.* **1998**, *11*, 535–538.
13. Zack, D. J.; Stempniak, M.; Wong, A. L.; Taylor, C.; Weisbart, R. H. *J. Immunol.* **1996**, *157*, 2082–2088.
14. Reichlin, M. *J. Autoimmun.* **1998**, *6*, 76–78.
15. Foster, M. H.; Kieber-Emmons, T.; Ohliger, M.; Madaio, M. P. *Immunol. Res.* **1994**, *13*, 186–206.
16. Adamus, G.; Machnicki, M.; Elerding, H.; Sugden, B.; Blocker, Y. S.; Fox, D. A. *J. Autoimmun.* **1998**, *11*, 523–533.
17. Rivadeneyra-Espinoza, L.; Ruiz-Arguelles, A. *J. Autoimmun.* **2006**, *26*, 52–56.
18. Park, J. S.; Kim, Y. T.; Chung, H. Y.; Beak, K.; Jang, Y. J. *Mol. Cells* **2001**, *11*, 55–63.
19. Ulrich, H. D.; Mundorff, E.; Santarsiero, B. D.; Driggers, E. M.; Stevens, R. C.; Schultz, P. G. *Nature* **1997**, *389*, 271–275.
20. Adamus, G. *Autoimmun. Rev.* **2003**, *2*, 63–68.
21. Ternynck, T.; Avrameas, A.; Ragimbeau, J.; Buttin, G.; Avrameas, S. *J. Autoimmun.* **1998**, *11*, 511–521.
22. Jang, Y. J.; Lecerf, J.-M.; Stollar, B. D. *Mol. Immunol.* **1996**, *33*, 197–210.
23. Mouratou, B.; Rouyre, S.; Guesdon, J.-L. *J. Immunol. Methods* **2002**, *269*, 147–155.
24. Jang, Y. J.; Park, K. S.; Chung, H. Y.; Kim, H. I. *Cancer Lett.* **2003**, *194*, 107–117.
25. Jeon, Y. E.; Seo, C. W.; Yu, E. S.; Lee, C. J.; Park, S. G. *Mol. Immunol.* **2007**, *44*, 827–836.